Evaluating modular parabolic solar concentrators for meeting the domestic hot water needs of Canada's northern remote Indigenous communities

Matthew Newport[1], Jean Duquette[1]
[1]Carleton University, Ottawa, Canada

Abstract

Diesel is a prominent heating fuel in Canada's northern Indigenous communities. Despite its many benefits, diesel use is both costly and highly polluting. A key strategy for displacing diesel involves switching to renewable technologies that harness solar energy. Modular parabolic solar concentrators are suitable for this purpose as they can be used to meet domestic hot water needs at the building level. This study describes the development of a modular two-axis parabolic solar concentrator model for residential hot water heating. Component sizes are optimized to meet the water heating needs of a hypothetical residential building located in the Canadian remote Indigenous community of Moose Factory, Ontario. Results show that the proposed system is a favourable approach to supplying domestic hot water to remote communities from both a technical and environmental standpoint with estimated % reductions in daily CO_2 emissions (relative to a diesel-based heater) of 69% and 91% on the coldest and warmest days of the year, respectively.

Introduction

According to a recent Canadian Energy Regulator report, approximately 178 Indigenous and remote northern communities in Canada are not connected to the continental electricity grid (Canada Energy Regulator, 2023). These communities predominantly depend on diesel for their energy needs due to their geographical separation from both the electrical grid and natural gas facilities. According to Natural Resources Canada, these isolated areas use upwards of 90 million litres of diesel each year solely for generating electricity. This figure does not include the diesel fuel used for heating purposes, which is estimated to be two to three times greater than that used for electricity generation (Lovekin & Heerema, 2019). While diesel is a stable source of energy, particularly in harsh cold weather conditions, offering consistent heat and power, it also presents several significant drawbacks. The cost of diesel, including its transportation to these isolated areas, is high, necessitating transportation by truck, barge, or aircraft. Some communities cannot be reached year-round, making air transport the only option, which can significantly increase costs. The unsubsidized cost to generate electricity in these communities can reach upwards of $3.19/kWh (Elasaraf, Jamil, & Pandey, 2021). The environmental impact of relying on diesel is also considerable, leading to local air pollution, emissions of greenhouse gasses, and the risk of fuel leaks and spills during transport or usage. Furthermore, the health effects on inhabitants in these areas are worrisome, with diesel emissions containing particulate matter that has been linked to cancer in animal studies and can cause immediate health issues like lung irritation and headaches (OSHA, 2013).

Current alternatives to diesel fuel for electricity generation and space heating include biomass, renewables, such as solar and wind, and geothermal. Solar thermal concentrators are a promising alternative that can help reduce the diesel dependency of remote communities. Around the world, solar concentrator systems have been used in remote communities for numerous applications like cooking, water distillation, domestic hot water (DHW) production, and space heating (Bhambare & Vishweshwara, 2022). Scheffler solar concentrators, designed by Wolfgang Scheffler, are a relatively recent development in the realm of solar concentrators. These concentrators are well suited for remote communities as they are cost effective and relatively simple to manufacture (Scheffler, 2006). The Scheffler design is highly beneficial as it includes a fixed focal point, a sun-tracking mechanism, and a flexible frame that can be adjusted to accommodate seasonal changes in solar declination. Furthermore, the design is such that no shadow is cast by the receiver onto the concentrator at any given time of the day (Reddy D. S. et al., 2018).

Literature Review

Scheffler concentrators have gained considerable traction in the field of solar energy in recent years. There exists a number of studies on all sizes of Scheffler concentrator, ranging from small (2 m^2) to large (16 m^2), for diverse applications.

These studies include comprehensive research on the usability, design optimization, and corresponding energy performance of these systems. For instance, Reddy et al. (2018) conducted a study in which they developed design

charts for facilitating rapid estimation of critical Scheffler design parameters such as section plane angles and concentration ratios, based on aperture area and focal length. This is particularly beneficial when manufacturing Scheffler concentrators to meet specific dimensional requirements. Building upon this study, Reddy and Khan (2019) conducted a modelling study proposing novel crossbar designs that aim to effectively eliminate errors in the concentrator profile, resulting in better efficiency and higher accuracy. Using an in-house ray tracing model, they found that even minor deviations in the shape of the concentrator had a substantial impact on performance. Their design enhancements resulted in reducing the error in the profile shape, and providing an improved image at the receiver. The versatility of Scheffler concentrators is demonstrated in its wide array of applications, from domestic cooking and water heating to industrial processes such as desalination. In their review study, Panchal et al. (2020) highlighted the suitability of Scheffler concentrators for medium-temperature applications due to their ability to maintain a constant temperature at the receiver, which is essential for processes requiring consistent heat. Chandak and Somani (2009) developed an experimental multi-effect desalination system using two 8 m^2 Scheffler concentrators to generate steam at 8 bar pressure. Their design included four distillation units to convert high-pressure steam into potable water. They achieved a distillate output of 6.5 L/m^2. Panchal and Sadasivuni (2018) experimentally showcased the integration of latent and sensible heat storage materials with a Scheffler cooking system and presented results for efficient and extended cooking times. They compared three different heat storage materials including pebbles, iron balls, and acetamide. Their results showed that when using pebbles and acetamide together, 70% of the stored heat was usable when the concentrator was not active. They also found that when using sensible and latent heat storage in combination, the payback period relative to a liquid propane gas cylinder was 30 months. Another experimental study by Kumar (2021) demonstrated the Scheffler concentrator's superior efficiency and concentration ratio compared to other conventional solar parabolic concentrator designs. The Scheffler concentrator achieved an efficiency of 59.28%, surpassing that of the other conventional designs by roughly 25%.

Typically, the efficiency of the concentrator component in a Scheffler solar thermal system ranges from about 80% to 100%, making the receiver the primary limiting factor in overall system efficiency (Nene et al., 2019). Most receiver designs discussed in the studies presented above are cavity-type receivers that do not include covers. The reason they don't have covers is that the medium to high temperatures typically desired are not compatible with glass materials. The lack of such a cover can greatly increase convection losses leading to reduced efficiencies in the receiver. This problem can potentially be addressed by using a smaller sized concentrator and combining it with a covered receiver design that uses a working fluid such as water to harness solar energy. This in turn can help maintain the receiver temperature within the operational range of glass.

The main objective of this study is to develop a novel covered receiver design for a 1.7 m^2 Sheffler concentrator that is used to heat domestic water in the northern remote Indigenous community of Moose Factory, Ontario. A secondary objective is to evaluate the system's daily output water temperature and corresponding CO_2 emission reductions relative to using diesel as the primary heating source. The following sections describe the fundamental Scheffler concentrator geometry, the modelling approach (MATLAB®) utilized to develop the covered receiver design, and the methods taken to evaluate overall system performance.

Methods

Proposed System

The proposed system, shown in Figure 1, is assumed to be located in the northern Indigenous community of Moose Factory, Ontario. Figure 1 shows how the Scheffler concentrator reflects solar rays towards the receiver. As the receiver warms up, heat is transferred to the domestic water circulating within, which then exits at the outlet. Flow is maintained in the system via the use of a centrifugal pump.

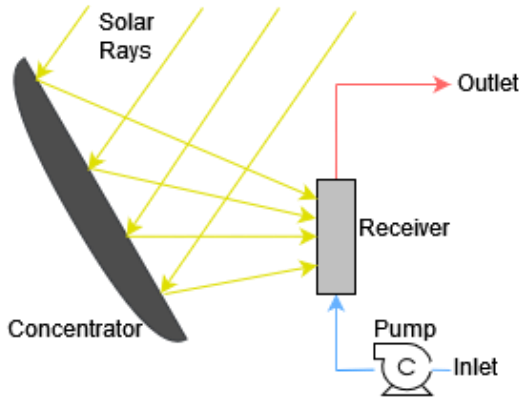

Figure 1: Schematic of proposed Scheffler concentrator domestic water heating system

Seasonal Variation of Concentrator Aperture Size

The Scheffler concentrator modeled in this study is designed following an approach outlined by Bhambare et al. (2022) that involves a simple reference parabola in three-dimensional space. Rotating this parabola about the y-axis results in a paraboloid and slicing the paraboloid surface with a cutting plane defines the parabolic concentrator section seen in Figure 2.

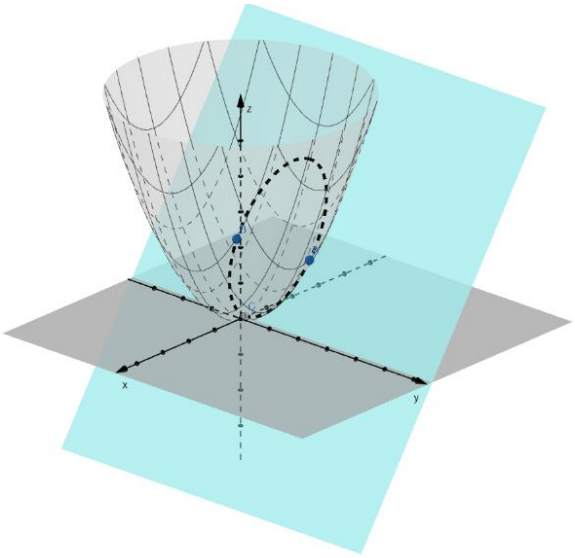

Figure 2: 3-D schematic of paraboloid with cutting plane defining the shape of the concentrator

Figure 3 depicts a two-dimensional view of the parabolic concentrator section. The cutting plane appears as a direct line intersecting the parabola at points A and B. Additionally, a point C is positioned on the parabola, where the tangent line at this point forms a 45-degree angle with the x-axis. The location of these points ensures that the solar rays at point C are deflected at a right angle, directing them horizontally toward the focal point, Z. The light path from point C to point Z serves as the daily axis of rotation around which the concentrator rotates for solar tracking purposes. To ensure the concentrator is structurally balanced, point C is positioned near its centre of gravity.

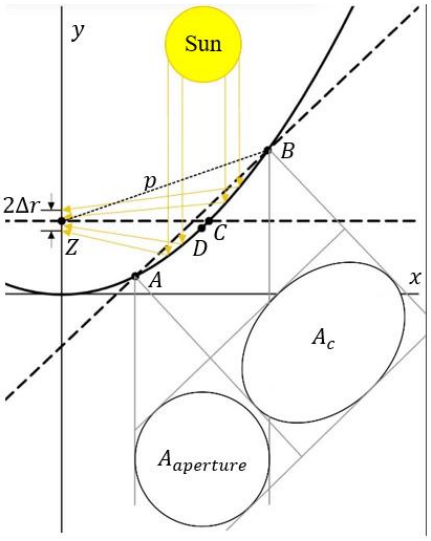

Figure 3: 2-D schematic of a Scheffler parabolic concentrator section showing points A, B, C, D, and Z, and areas A_c and $A_{aperture}$ (adapted from Bhambare et al. (2022))

The Scheffler design is unique in that it allows for seasonal shape adjustments of the concentrator. These shape adjustments allow the concentrator to operate more efficiently on an annual basis by capturing more sunlight. Point D in Figure 3 is the location of the concentrator's central pivot point. The position of point D changes throughout the year as the shape of the concentrator changes, allowing the position of point Z to remain fixed (Bhambare & Vishweshwara, 2022). To calculate the relative position of point D as a function of solar declination, a rotation matrix is used. Further details regarding the geometry of the Scheffler concentrator can be obtained from Bhambare et al. (2022).

Any seasonal adjustments to the concentrator's shape also affect the aperture area (m^2) as follows:

$$A_{aperture} = A_c \cos\left(D_{tangent} \pm \frac{\delta}{2}\right) \quad (1)$$

where A_c is the concentrator area (m^2), $D_{tangent}$ is the angle between the tangent line at point D relative to the x-axis (which remains constant on an annual basis), and δ is the solar declination angle (degrees). Throughout the year, the solar declination angle varies between ± 23.45 degrees.

Receiver Design

The size of the receiver is determined by the radius of the image formed at the focus of the concentrator by the reflected beam. Since the Sun has a finite size, the solar rays that reach the concentrator are not perfectly parallel.

Alongside the Sun's finite angular dimensions, several other factors contribute to the reflected beam (Stine & Geyer, 2010). These include discrepancies in the concentrator's shape, reflections that are non-specular, inaccuracies with tracking, and misalignments of the receiver. These deviations can be treated as random and quantified in a probabilistic manner. The collective impact of these factors is assessed in this study via statistical methods. It should be noted that the sunlight intensity is not normally distributed, however for simplicity, it can be approximated as such (Stine & Geyer, 2010). The image radius (m) formed at the focus (shown in Figure 3) is given by

$$\Delta r = 2p \tan\left(\frac{n\emptyset}{2}\right) \quad (2)$$

where p (m) is the distance of the edge of the parabola to the focus, $\emptyset$ (radians) is the net error considering both one-dimensional (*i.e.*, slope, tracking, and alignment) and two-dimensional (*i.e.*, Sun diameter, and specular) errors, and n is the total number of standard deviations considered (both positive and negative). The distance from the edge of the parabola to the focus is the distance from point B to point Z. The net error is obtained from a study conducted by Stine (2010). The total number of standard deviations is assumed to be three (*i.e.*, n = 6) since this value corresponds to roughly 99.73% of the concentrated rays being captured by the receiver aperture (Stine & Geyer, 2010).

Therefore, the solar irradiance incident on the receiver (W/m^2) is expressed as

$$S = 0.9973R\left(\frac{IA_{aperture}}{A_r}\right) \quad (3)$$

where I (W/m^2) is the incident direct normal irradiance on the concentrator and R is the reflectivity of the concentrator. The receiver is designed as a flat plate collector with a glass cover as seen in the cross-section in Figure 4. The receiver includes nine parallel copper pipes, each with a diameter D (m), that are spaced (midpoint to midpoint) by a distance W (m). The absorber plate (with thickness t_p (m)) is made of copper and is painted with black chromium. The glass cover, fiberglass insulation, and aluminum outer casing have thicknesses of t_c (m), L_i (m), and t_{case} (m), respectively. The outer casing and the glass cover provide insulation from convective losses and the fibreglass insulation provides insulation from conductive losses. Since the receiver is square shaped (with dimensions of length l_r (m), width w_r (m), and thickness t_r (m), as indicated in Figure 5), its length and width are sized to exactly accommodate the area of the focused solar image, such that

$$l = w = 2\Delta r \quad (4)$$

Therefore, the area of the projected solar image on the glass cover of the receiver (m^2) is given by:

$$A_r = \pi\Delta r^2 \quad (5)$$

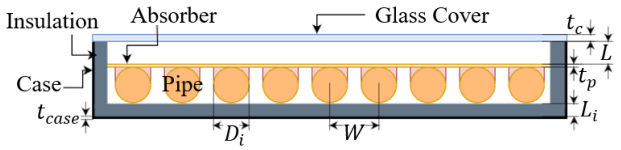

Figure 4: Cross-section of the receiver showing individual components

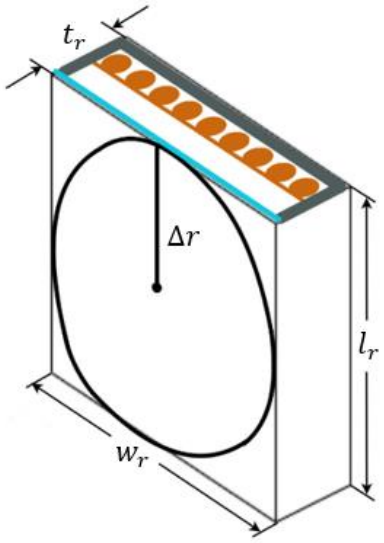

Figure 5: Isometric view of the receiver showing focused image reflected by the concentrator

The receiver model is developed in the MATLAB® environment and is largely based on a collector model derived by Hottel and Whillier (1958). The following assumptions are taken in formulating the model: steady state conditions, water is the working fluid; fluid flow is fully developed, one-dimensional, and incompressible; heat flow through the glass cover, absorber, and insulation is one-dimensional; material properties of the collector are constant in time and space, and temperature independent. The usable energy (*i.e.*, the energy collected by the receiver and transferred to the working fluid) is expressed as (Duffie et al., 2020):

$$Q_u = A_r F_r\big(S - U_L(T_{in} - T_{amb})\big) \quad (6)$$

where T_{in} (K) and T_{amb} (K) are the inlet fluid temperature and the ambient air temperature, respectively. U_L (W/ m^{2}K) is the overall heat loss coefficient given by (Duffie et al., 2020):

$$U_L = U_b + U_e + U_T \quad (7)$$

where U_b (W/m^{2}K), U_e (W/m^{2}K),) and U_T (W/m^{2}K) are the back, edge, and top heat loss coefficients of the receiver, respectively. The back and edge heat loss coefficients determine the conductive heat losses through the insulation of the receiver and are calculated using the following expressions (Duffie et al., 2020):

$$U_b = {k_i}/{L_i} \quad (8)$$

$$U_e = \frac{k_i A_e}{L_i A_b} \quad (9)$$

where k_i (W/mK), A_e (m^2), and A_b (m^2) represent the thermal conductivity of the insulation, the edge area, and the back cover area, respectively. The top heat loss coefficient of the receiver is calculated using the following relation which requires an iterative solution method (Duffie et al., 2020):

$$U_T = \left(\frac{1}{h_{c,p-c} + h_{r,p-c}} + \frac{1}{h_w + h_{r,c-a}}\right)^{-1} \quad (10)$$

The parameters $h_{r,p-c}$ (W/m^{2}K), $h_{r,c-a}$ (W/m^{2}K), $h_{c,p-c}$ (W/m^{2}K), and h_w (W/m^{2}K) represent the radiative coefficient from the plate to the cover, the radiative coefficient from the glass cover to the surroundings, the convection heat loss coefficient from the plate to the cover, and the wind coefficient, respectively, and are expressed as (Duffie et al., 2020):

$$h_{r,p-c} = \frac{\sigma\left(T_p^2 + T_c^2\right)\left(T_p + T_c\right)}{\frac{1}{\varepsilon_p} + \frac{1}{\varepsilon_c} - 1} \quad (11)$$

$$h_{r,c-a} = \varepsilon_c \sigma (T_c^2 + T_s^2)(T_c + T_s) \quad (12)$$

$$h_{c,p-c} = \frac{Nu\ k}{L} \quad (13)$$

$$h_w = 3.9v_w + 5.62 \quad (14)$$

where σ (W/m^{2}K^4), T_p (K), T_c (K), ε_p and ε_c, k (W/mK), v_w (m/s), and Nu in Equations 11, 13, and 14 are the Boltzmann constant, the plate temperature, the cover temperature, the plate and cover emissivity, the thermal conductivity of air, the wind velocity, and the dimensionless Nusselt number, respectively. The Nusselt number is given by (Duffie et al., 2020):

$$Nu = 1 + 1.44\left[1 - \frac{1708(sin1.8\beta)^{1.6}}{Ra\ cos\beta}\right]\left[1 - \frac{1708}{Ra\ cos\beta}\right] + \left[\left(\frac{Ra\ cos\beta}{5830}\right)^{1/3} - 1\right]^{+} \quad (15)$$

where Ra and β represent the Rayleigh number and the receiver tilt angle, respectively. The $+$ exponent signifies that the values in the square brackets must be positive, or zero if negative.

In Equation 16, T_s (K) represents the effective sky temperature which is approximated using the following equation developed by Berdahl and Martin (1984):

$$T_s = T_{amb}\left(0.711 + 0.0056T_{dp} + 0.000073T_{dp}^2 + 0.013cos(15t)\right)^{1/4} \quad (16)$$

where T_{dp} (K) is the dew point temperature and t is the time in hours from midnight. The parameter T_c (K), also from Equation 11, represents the cover temperature, which is a function of the mean plate temperature, T_{pm} (K), as follows (Duffie et al., 2020):

$$T_c = T_{pm} - \frac{\left(U_T\left(T_{pm} - T_{amb}\right)\right)}{h_{r,p-c} + h_{c,p-c}} \quad (17)$$

$$T_{pm} = T_{in} + \frac{Q_u}{A_r F_R U_L}(1 - F_R) \quad (18)$$

F_r is the heat removal factor, which is described by the following equation set (Duffie et al., 2020):

$$F_R = \frac{\dot{m}C_p}{A_r U_L F'}\left[1 - exp\left(-\frac{A_r U_L F'}{\dot{m}C_p}\right)\right] \quad (19)$$

$$F' = \frac{1/U_L}{W\left[\frac{1}{U_L[D + F(W + D)]} + \frac{1}{\pi D_i h_{fi}}\right]} \quad (20)$$

$$F = \frac{tanh\left[\sqrt{\frac{U_L}{k_p t_p}}\frac{(W - D)}{2}\right]}{\sqrt{\frac{U_L}{k_p t_p}}\frac{(W - D)}{2}} \quad (21)$$

where F', F, $\dot{m}$ (kg/s), C_p (J/kgK), D_i (m), h_{fi} (W/m^{2}K), and k_p (W/mK) represent the receiver efficiency factor, the fin efficiency factor, the mass flowrate of the working fluid in the pipes, the specific heat capacity of the working fluid, the hydraulic diameter of the pipe, the pipe internal heat transfer coefficient, and the plate thermal conductivity, respectively. When solving the model formulation presented above, an iterative method is used to allow the convergence of plate and cover temperatures to achieve an accurate energy balance.

A summary of the fixed parameter values utilized in the analysis is provided in Table 1.

Table 1: Parameter values of the receiver design

Parameter	Description	Value	Unit
A_c	Area of concentrator	1.7	m^2
$D_{tangent}$	Angle of tangent line at point D	43.223	Degrees
Δr	Radius of image on receiver	0.1654	m^2
n	Standard deviations of error	6	-
R	Concentrator reflectivity	0.95	-
A_r	Area of receiver	0.0273	m^2
l_r	Length of receiver	0.1654	m
w_r	Width of receiver	0.1654	m
t_r	Thickness of receiver	0.063	m
k_i	Thermal conductivity of insulation	0.044	W/mK
L_i	Thickness of insulation	0.1	m
A_e	Edge area of receiver	0.01965	m^2
A_b	Back area of receiver	0.02736	m^2
σ	Boltzmann constant	5.6e-10	W/m^{2}K^4
ε_p	Emissivity of absorber plate	0.95	-
ε_c	Emissivity of cover	0.89	-
k	Air conductivity	0.0293	W/mK
L	Air gap length	0.025	m
t_p	Plate thickness	0.002	m
t_c	Cover thickness	0.006	m
t_{case}	Case thickness	0.005	m
D	Pipe outer diameter	0.015	m
W	Pipe spacing	0.02	m
D_i	Pipe hydraulic diameter	0.01125	m
h_{fi}	Pipe internal heat transfer	194.54	W/m^{2}K
k_p	Plate conductivity	401	W/mK
C_p	Specific heat capacity of water	4184	J/kgK
$\emptyset$	Net error	0.0067	radians

Estimation of Water Outlet Temperature

The water outlet temperature (°C) is given by (Duffie et al., 2020):

$$T_{out} = \left(T_{in} - T_{amb} - \frac{S}{U_L}\right)exp\left(-\frac{U_L A_r F'}{mC_p}\right) + T_{amb} + \frac{S}{U_L} \quad (22)$$

In the current study, T_{out} is calculated on an hourly basis on both the coldest winter day (February 28th) and warmest summer day (July 1st) of the 2020 reference year. This output represents the daily domestic water temperature

profile that can be achieved in Moose Factory, ON, while using the proposed Scheffler parabolic concentrator to heat water from a fixed inlet temperature at a constant mass flow rate. The inlet temperature for February 28th is assumed to be equal to the average daily mains temperature in Ottawa during the month of February. The inlet temperature for July 1st is assumed to be equal to the Ottawa River average temperature during the month of July (City of Ottawa, 2024; Sea Temperature, 2023). The mass flow rate is determined to maximize the collector efficiency and to produce the daily hot water requirement for a typical 4-person Canadian home (NRCan, 2012).

Table 2 shows the values of the fixed input parameters used in the analysis. Figure 6 shows the daily variation in ambient temperature and solar irradiance for the two days mentioned above. The information is sourced from a CWEC weather file specific to Moose Factory Island (Climate One Building, 2023).

Table 2: Fixed input parameters used in estimation of water outlet temperature

Parameter	Description	Value	Unit
$\dot{m}$	Mass flow rate	0.005	kg/s
T_{in} (February 28th)	Inlet water temperature	5	°C
T_{in} (July 1st)	Inlet water temperature	19.4	°C
$A_{aperture}$ (February 28th)	Aperture area	1.309	m^2
$A_{aperture}$ (July 1st)	Aperture area	1.062	m^2

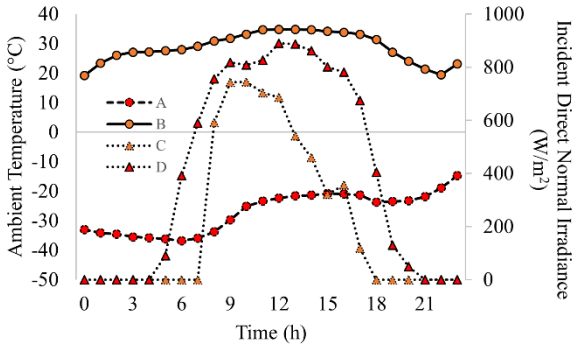

Figure 6: Ambient temperature and incident direct normal irradiance on February 28th (A and C) and July 1st (B and D), respectively

Estimation of CO_2 Emission Reductions

The daily CO_2 emission reductions from using the proposed Scheffler parabolic concentrator to heat water are given by

$$\%_{red_daily} = \left(\frac{E_{daily_sup}}{E_{daily_req}}\right) \times 100\% \qquad (23)$$

where E_{daily_sup} (J) and E_{daily_req} (J) are the daily energy supplied by the Scheffler parabolic concentrator and the daily energy required to heat water from T_{in} to T_{set} using a conventional diesel-based heater, respectively. The daily energy supplied by the concentrator is expressed as

$$E_{daily_sup} = \sum_{i=5}^{20} m_{water_hourly} C_p \left(T_{out_i} - T_{in_i}\right) \qquad (24)$$

where i represents the hour of the day, and m_{water_hourly} is the mass of water (kg) heated by the concentrator at every hour. The daily energy required to heat water from T_{in} to T_{set} using a conventional diesel-based heater is given by

$$E_{daily_req} = m_{water_daily} C_p (T_{set} - T_{in}) \qquad (25)$$

where m_{water_daily} is the mass of water (kg) heated by the concentrator during its daily operational period.

The following assumptions are taken:

- The concentrator is operated for 16 hours/day on July 1st and February 28th (*i.e.*, from 5 h to 20 h). This time period corresponds to the daily insolation hours on July 1st. It is also the time required to produce 288 L of hot water which is approximately the daily DHW requirement for a typical 4-person Canadian home (NRCan, 2012).
- The DHW setpoint temperature T_{set} is 60°C.
- A conventional diesel-based heater is used to heat water to T_{set} when the concentrator is unable to reach this temperature.
- The input parameters shown in Table 2 are used in the analysis.
- Reductions in energy consumption from using the concentrator are directly proportional to reductions in CO_2 emissions.

CO_2 emission reductions are estimated for both February 28th and July 1st of the reference year.

Model Verification

The proposed model is verified by completing energy balance checks using the temporal outputs from the integrated system components to ensure that energy conservation is maintained. Manual calculations are also carried out using varied input conditions to verify that the model's predicted values are as expected. Differences of less than 2% are found at any given time which are considered to be negligible.

Results and Discussion

The daily water outlet temperature is shown in Figures 7 and 8 for the coldest winter day (February 28th) and the warmest summer day (July 1st) in Moose Factory, ON, respectively.

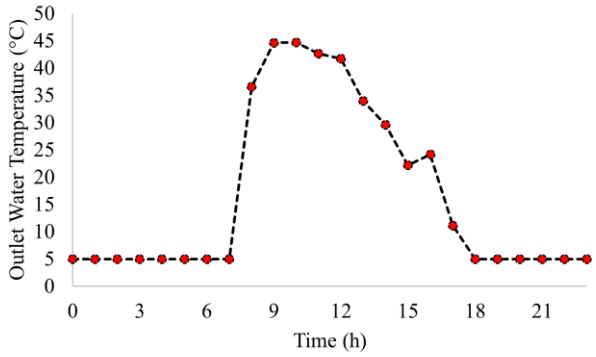

Figure 7: Outlet water temperature on the coldest day (February 28th) in Moose Factory, ON

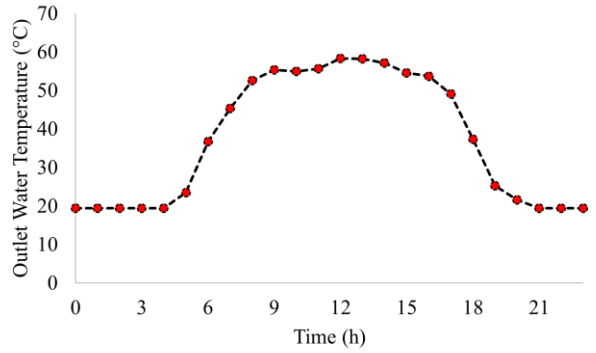

Figure 8: Outlet water temperature on the warmest day (July 1st) in Moose Factory, ON

On the warmest (and longest) day, the outlet water temperature increases to roughly 60°C, whereas, on the coldest (and shortest) day, the outlet water temperature increases to approximately 45°C. This difference in maximum daily temperature (*i.e.*, 15°C) is relatively small considering the average daily ambient temperature on February 28th is roughly 40°C lower than on July 1st. Moreover, the inlet water temperature on February 28th is about 15°C lower than on July 1st. This result is mainly attributed to the low heat losses of the receiver (since its surface area is small and it includes a cover). It is also partly attributed to there being a larger aperture area in February than in July. The proposed Scheffler concentrator system is therefore a potentially attractive option for providing DHW to the residents of northern remote communities such as Moose Factory due to its relatively stable annual water outlet temperatures, despite the challenging weather conditions that are present in these areas.

The corresponding % reductions in daily CO_2 emissions from using the proposed Scheffler parabolic concentrator to heat water relative to a diesel-based heater are shown in Table 3 for both days mentioned above.

Table 3: Estimated % reductions in daily CO_2 emissions

Day of Year	$\%_{red_daily}$
February 28th	69
July 1st	91

Table 3 shows that the % reductions in daily CO_2 emissions are greater on July 1st than on February 28th. This is due to the increased insolation hours, ambient temperature, and inlet water temperature in July relative to February which contribute to more efficient solar water heating. This result shows that the proposed Scheffler concentrator system can be used effectively year-round to displace CO_2 emissions from the combustion of diesel fuel. Making this switch can have a significant impact on the health and wellbeing of community members.

Although the proposed system model produces promising results, the following simplifications are made in creating it which should not be overlooked:

- Steady state conditions are used which ignore transient phenomena such as thermal inertia and material temperature dependence. This can lead to inaccuracies in predicting the performance of the system under dynamic conditions.
- Water is used as the working fluid which may be unrealistic in northern communities where temperatures often fall below freezing. A better option may be to consider a glycol water mix and a separate heat exchanger to decouple the working fluid from the domestic hot water.
- The receiver has a square shape which introduces some inefficiency in the design because the concentrated image formed upon its surface is circular.
- Hot water storage is not considered in the model. Adding a sensible hot water storage tank with variable flow rate control would improve the accuracy and performance of the system.
- No basis of comparison is provided. A comparative analysis between the proposed system and a traditional flat plate collector of similar size would provide useful information regarding potential cost and performance trade-offs.

Despite these limitations, the proposed Scheffler parabolic concentrator holds promise as a sustainable and low-cost water heating solution. This study serves as an initial step in a larger scale project aimed at reducing diesel dependency for residential heating applications in Canada's northern remote Indigenous communities.

Conclusion

In this study, a model was developed in MATLAB® of a Scheffler concentrator coupled to a unique receiver design for the purpose of supplying domestic hot water to a hypothetical residential building located in the Canadian remote Indigenous community of Moose Factory, Ontario. Daily outlet temperatures were calculated for the coldest (February 28th) and warmest (July 1st) days of the reference year. Results showed that daily outlet temperatures of

roughly 45ºC and 60ºC could be attained for each of these days, respectively. Additionally, the % reductions in daily CO_2 emissions from using the proposed system to heat water relative to a diesel-based heater were estimated. Results showed that CO_2 emissions could potentially be reduced by 69% and 91% for the same days mentioned above in the stated order. The findings of this study can be extended to other remote Indigenous communities in Canada that are faced with similar challenges.

References

Berdahl, P., & Martin, M. (1984). Emissivity of Clear Skies. *Solar Energy*, 663-664. doi:https://doi.org/10.1016/0038-092x(84)90144-0

Bhambare, P. S., & Vishweshwara, S. C. (2022). Design aspects of a fixed focus type Scheffler concentrator and its receiver for its utilization in thermal processing units. *Energy Nexus, 7*, 100-103. doi:https://doi.org/10.1016/j.nexus.2022.100103

Canada Energy Regulator. (2023). *Market Snapshot*. Retrieved from Clean energy projects in remote indigenous and northern communities

Chandak, A., & Somani, K. (2009). Design of Multistage Evaporators for Integrating with Scheffler Solar Concentrators for Food Processing Applications. *Proceedings of International Solar Food Processing Conference*.

City of Ottawa. (2024). *Drinking Water*. Retrieved from City of Ottawa

Climate One Building. (2023). *Climate/Weather Data Sources*. Retrieved from Climate.OneBuilding.Org

Duffie, J. A., Beckman, W., & Blair, N. (2020). Solar Engineering of Thermal Processes, Photovoltaics and Wind. doi:https://doi.org/10.1002/9781119540328

Elasaraf, H., Jamil, M., & Pandey, B. (2021). Techno-Economic Design of a Combined Heat and Power Microgrid for a Remote Community in Newfoundland Canada. *IEEE Access, 9*, 91548-91563.

Hottel, H. C., & Whillier, A. (1958). Evaluation of Flat-plate Collector Performance. *Transactions of the Conference on the Use of Solar Energy*.

Kumar, A. (2021). Experimental investigation of a Scheffler reflector for the medium temperature applications. *Journal of Thermal Engineering*. doi:https://doi.org/10.18186/thermal.978197

Lovekin, D., & Heerema, D. (2019). *Diesel, renewables, and the future of Canada's remote communities*. Retrieved from Pembina

Munusamy, A., Barik, D., Sharma, P., Medhi, B. J., & Bora, B. J. (2022). Performance analysis of parabolic type solar water heater by using copper-dimpled tube with aluminum coating. *Comtemporary Advancement in Solar Energy Engineering*. doi:https://doi.org/10.1007/s11356-022-25071-5

Nene, A., Ramachandran, S., & Suyambazhahan, S. (2019). Effect of Wind Flow on Convective Heat Losses from Scheffler Solar Concentrator Receivers. *Journal of the Institution of Engineers (India) Series C*, 737-745. doi:https://doi.org/10.1007/s40032-018-0463-5

NRCan. (2012). Water Heater Guide.

OSHA. (2013). *Diesel Exhaust*. Retrieved from Occupational Safety and Health Administration

Panchal, h., & Sadasivuni, K. (2018). Investigation and performance analysis of Scheffler reflector solar cooking system integrated with sensible and latent heat storage materials. *International Journal of Ambient Energy*, 1096-1105. doi:https://doi.org/10.1080/01430750.2018.1501754

Panchal, H., Patel, J., Parmar, k., & Patel, M. (2020). Different applications of Scheffler reflectors for renewable energy: a comprehensive review. *International Journal of Ambient Energy, 41*, 716-728. doi:https://doi.org/10.1080/01430750.2018.1472655

Reddy, D. S., Khan, M. K., Alam, M. Z., & Rashid, H. (2018). Design charts for Scheffler Reflector. *Solar Energy, 163*, 104-112. doi:https://doi.org/10.1016/j.solener.2018.01.081

Reddy, D., & Khan, M. (2019). Design and ray tracing of multifaceted Scheffler reflector with novel crossbars. *Solar Energy*. doi:https://doi.org/10.1016/j.solener.2018.01.081

Scheffler, W. (2006). Introduction to the revolutionary design of Scheffler reflectors. *Proc. International Conference on Solar Cookers*.

Sea Temperature. (2023). *Water temperature in Ottawa*. Retrieved from Sea Temperature: https://seatemperature.info/ottawa-water-temperature.html

Statistics Canada. (2021). *Census Profile, 2021 Census of Population*. Retrieved from Statisitcs Canada

Stine, W., & Geyer, M. (2010). Power from the Sun. Retrieved from www.loc.gov/item/lcwaN0004585/